AD-A129 555 CRACK INITIATION AND PROPAGATION IN METALS IN LIQUID MERCURY USING FRACTURE MECHANICS(U) ARMY ARMAMENT RESEARCH AND DEVELOPMENT COMMAND WATERVLIET NY L.. 1/1

UNCLASSIFIED J A KAPP MAR 83 F/G 11/6 NL

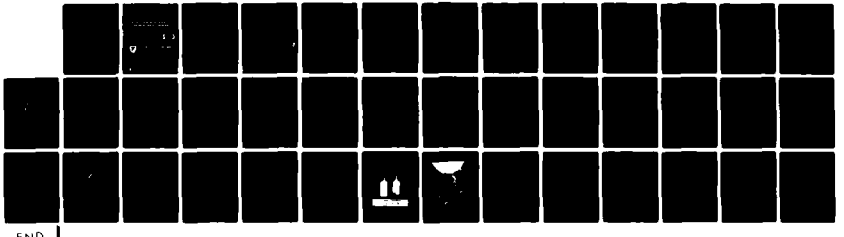

END
DATE FILMED
7 83
DTIC

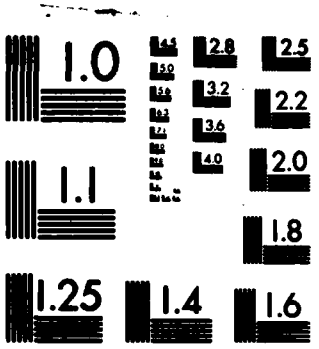

12

AD

TECHNICAL REPORT ARLCB-TR-83007

CRACK INITIATION AND PROPAGATION IN METALS IN LIQUID MERCURY USING FRACTURE MECHANICS

J. A. KAPP

MARCH 1983

US ARMY ARMAMENT RESEARCH AND DEVELOPMENT COMMAND
LARGE CALIBER WEAPON SYSTEMS LABORATORY
BENET WEAPONS LABORATORY
WATERVLIET N.Y. 12189

DISCLAIMER

The findings in this report are not to be construed as an official Department of the Army position unless so designated by other authorized documents.

The use of trade name(s) and/or manufacture(s) does not constitute an official indorsement or approval.

DISPOSITION

Destroy this report when it is no longer needed. Do not return it to the originator.

SECURITY CLASSIFICATION OF THIS PAGE (When Data Entered)

REPORT DOCUMENTATION PAGE	READ INSTRUCTIONS BEFORE COMPLETING FORM
1. REPORT NUMBER: ARLCB-TR-83007	2. GOVT ACCESSION NO.: AD-A129555
3. RECIPIENT'S CATALOG NUMBER	
4. TITLE (and Subtitle): CRACK INITIATION AND PROPAGATION IN METALS IN LIQUID MERCURY USING FRACTURE MECHANICS	5. TYPE OF REPORT & PERIOD COVERED: Final
	6. PERFORMING ORG. REPORT NUMBER
7. AUTHOR(s): J. A. Kapp	8. CONTRACT OR GRANT NUMBER(s)
9. PERFORMING ORGANIZATION NAME AND ADDRESS: US Army Armament Research & Development Command, Benet Weapons Laboratory, DRDAR-LCB-TL, Watervliet, NY 12189	10. PROGRAM ELEMENT, PROJECT, TASK AREA & WORK UNIT NUMBERS: AMCMS No. 61110191A0011, DA Project No. 1L161101A9A, PRON No. 1A2231491A1A
11. CONTROLLING OFFICE NAME AND ADDRESS: US Army Armament Research & Development Command, Large Caliber Weapon Systems Laboratory, Dover, NJ 07801	12. REPORT DATE: March 1983
	13. NUMBER OF PAGES: 33
14. MONITORING AGENCY NAME & ADDRESS(if different from Controlling Office)	15. SECURITY CLASS. (of this report): UNCLASSIFIED
	15a. DECLASSIFICATION/DOWNGRADING SCHEDULE

16. DISTRIBUTION STATEMENT (of this Report)

Approved for public release; distribution unlimited

17. DISTRIBUTION STATEMENT (of the abstract entered in Block 20, if different from Report)

18. SUPPLEMENTARY NOTES

Presented at 1982 Fall AIME Meeting, St. Louis, MO, October 1982.
Published in proceedings of the meeting.

19. KEY WORDS (Continue on reverse side if necessary and identify by block number)

Fracture
Fatigue
Fracture Mechanics
Liquid Metal Embrittlement

20. ABSTRACT (Continue on reverse side if necessary and identify by block number)

Fracture mechanics is a useful tool in the study of sub-critical crack growth. This report presents a summary of the results of several recent fracture mechanics studies of liquid metal embrittlement. Specific topics include crack growth measurements under cyclic loading conditions in 6061-T651 alloy embrittled by liquid mercury. The effect of mean stress on fatigue crack growth in a high strength-low alloy steel in mercury is discussed. Crack →

(CONT'D ON REVERSE)

DD FORM 1 JAN 73 1473 EDITION OF 1 NOV 65 IS OBSOLETE

UNCLASSIFIED

SECURITY CLASSIFICATION OF THIS PAGE (When Data Entered)

20. ABSTRACT (CONT'D)

growth studies under static loading conditions at various temperatures in both 6061-T651 aluminum and 70/30 alpha brass embrittled by mercury are also presented. Finally, some experiments on mercury wetted 70/30 alpha brass in Mode III loading (pure shear) are presented. The results are discussed in relation to transport mechanisms.

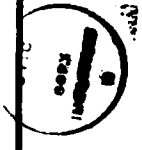

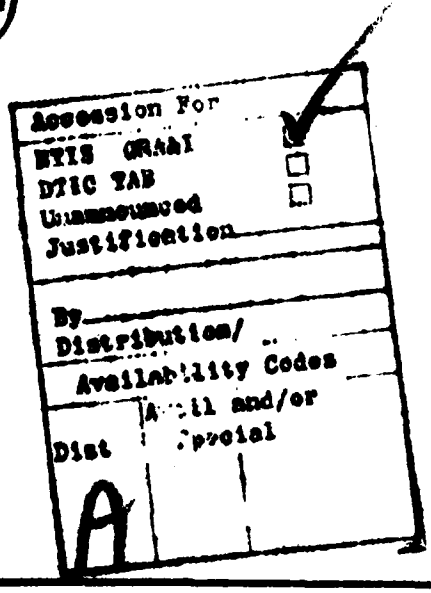

TABLE OF CONTENTS

TABLES

LIST OF ILLUSTRATIONS

ACKNOWLEDGEMENTS

The author wishes to thank Mr. C. Rickard for his assistance in the preparation of the metallographic results presented, Ellen Fogarty for manuscript preparation, and Dr. M. H. Kamdar for his suggestions.

INTRODUCTION

Fracture mechanics has proven very helpful in the understanding of many environmentally assisted fracture phenomena.[1,2] Extensive use of fracture mechanics has been used in several recent studies of liquid metal embrittlement at Benet Weapons Laboratory[3,4] and Rensselaer Polytechnic Institute.[5] This report is a brief review of these recent studies. Also presented are the results of some crack initiation Mode III (pure shear) tests.

EXPERIMENTAL PROCEDURES

Specimens

The specimens used to generate the results presented in this study are shown in Figure 1. Crack growth rate measurements were obtained using both the short double cantilevered beam (SDCB) specimen and the bend specimen. The Mode III crack initiation tests were performed using the notched torsion specimen. The stress intensity factors, K_I for the SDCB and bend specimens, K_{III} for the torsion specimens, were obtained from the handbook by Tada et al.[6] The crack mouth opening displacement (CMOD) solutions for the SDCB and

---

[1]Clark, W. G. Jr., "Effect of Temperature and Pressure on Hydrogen Cracking in High Strength Type 4340 Steel," J. Materials for Engineering Systems, Vol. 1, June 1979, pp. 33-40.

[2]Wei, R. P., "On Understanding Environment-Enhanced Fatigue Crack Growth - A Fundamental Approach," ASTM STP 675, J. T. Fong, Ed., American Society for Testing and Materials, 1979, pp. 816-840.

[3]Kapp, J. A., "The Combined Effects of Mean Stress and Aggressive Environments on Fatigue Crack Growth," ARLCB-TR-82012, ARRADCOM, Benet Weapons Laboratory, Watervliet, NY, May 1982.

[4]Kamdar, M. H., "The Role of Liquid in the Mechanics of Crack Growth in LME," in progress.

[5]Kapp, J. A., "Crack Growth in Mercury Embrittled Aluminum Alloys Under Static and Cyclic Loading Conditions," Ph.D. Thesis, Rensselaer Polytechnic Institute, Troy, NY, 1982.

[6]Tada, H., Paris, P. C., and Irwin, G. R., The Stress Analysis of Cracks Handbook, Del Research Corporation, Hellertown, PA, 1973.

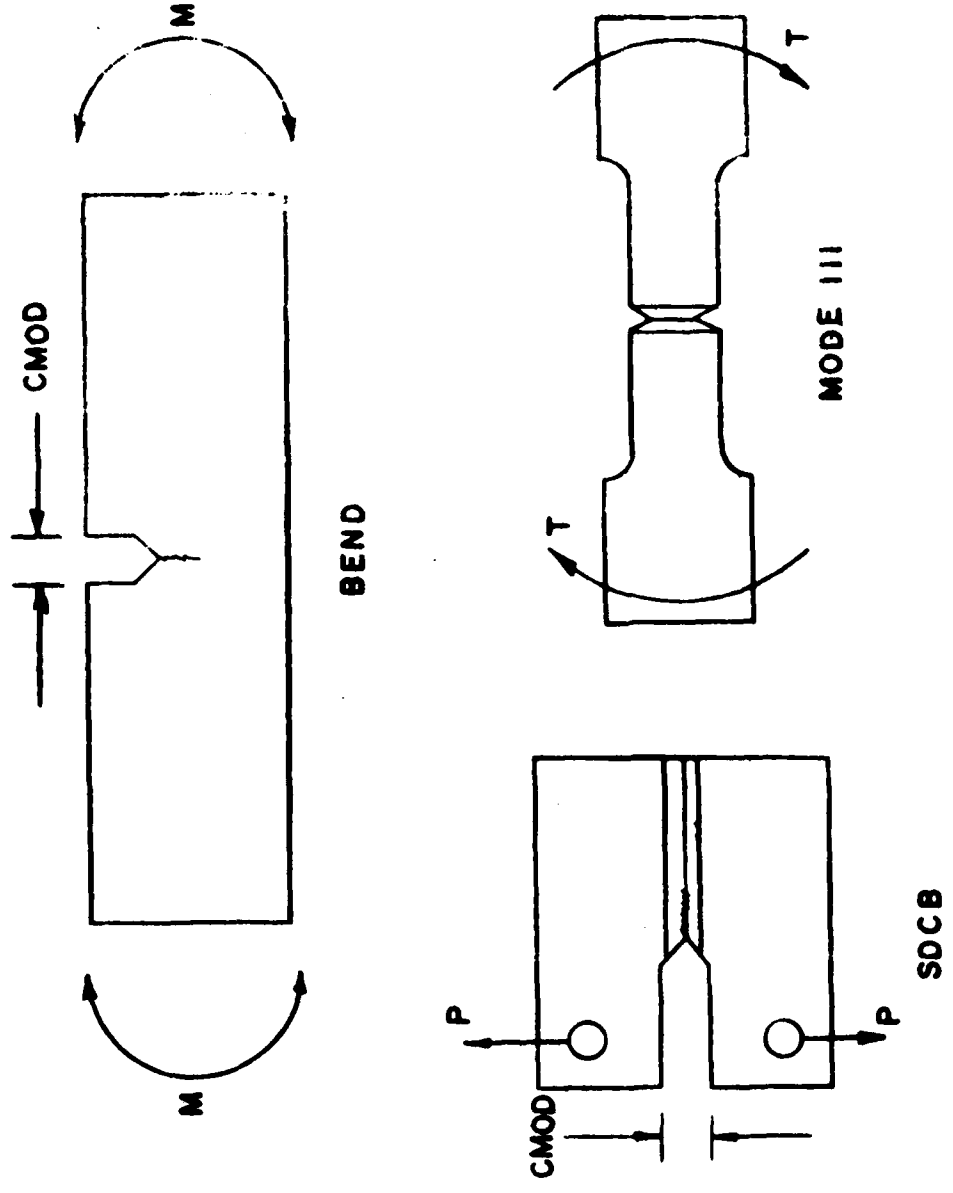

Figure 1. The three specimens used in the various crack growth and crack initiation studies.

the bend specimens were also given in Reference 6.

Crack growth was measured using the so called "Compliance" method.[7] Both the applied load and CMOD were measured simultaneously. Combining these measurements with the analytical solutions for the CMOD, the crack lengths were calculated. Once the crack length was determined, the crack growth rate and the stress intensity factor were calculated. In the Mode III tests crack initiation was determined from the torque-twist diagram and subsequent metallographic examination.

Materials

A total of three materials were studied in the various programs summarized here: the aluminum alloy 6061-T651, a Ni-Cr-Mo steel, and 70/30 alpha brass. The mechanical properties of all these materials are listed in Table I. The most extensive study was performed on the 6061-T651 alloy.[5] Crack growth rates were measured under cyclic loading conditions at two frequencies, under two static loadings, fixed displacement or fixed load; and at several temperatures under all loading conditions. The testing of the 70/30 alpha brass included static loading crack propagation measurements at various temperatures,[4] and the Mode III crack initiation studies. The

---

[4]Kamdar, M. H., "The Role of Liquid in the Mechanics of Crack Growth in LME," in progress.

[5]Kapp, J. A., "Crack Growth in Mercury Embrittled Aluminum Alloys Under Static and Cyclic Loading Conditions," Ph.D. Thesis, Rensselaer Polytechnic Institute, Troy, NY, 1982.

[6]Tada, H., Paris, P. C., and Irwin, G. R., The Stress Analysis of Cracks Handbook, Del Research Corporation, Hellertown, PA, 1973.

[7]Yoder, G. R., Cooley, L. A., and Crooker, T. W., "Procedures for Precision Measurement of Fatigue Crack Growth Rate Using Crack-Opening Displacement Techniques," ASTM STP 738, S. J. Hudak and R. J. Bucci, Eds., American Society for Testing and Materials, 1981, pp. 85-102.

Ni-Cr-Mo steel study[3] was an attempt to model the effects of mean stress on fatigue crack growth. In all studies, the embrittling liquid metal was mercury.

TABLE I. MECHANICAL PROPERTIES OF THE MATERIALS STUDIED

Material	0.1% σ_{ys} (MPa)	σ_{UTS} (MPa)	% Elongation	% RA
6061-T651	282.0	312.3	14.3	35.7
Ni-Cr-Mo Steel	1059	1149	14.3	40.7
70/30 Alpha Brass	218.6	366.1	48.6	70.7

Wetting Procedure

In the crack growth studies, the specimens were wetted with mercury and cycled to failure in the fatigue crack growth tests. The static loading specimens were first cyclically loaded to produce an embrittled crack, then tested to failure. For the Mode III crack initiation tests, care was taken to wet only the notch tip, where the stresses were pure Mode III, or pure shear.

Wetting of the brass samples was accomplished by coating the area to be wetted with an aqueous solution of mercurous nitrate. After a thin film of mercury was deposited by chemical displacement, a few drops of pure liquid mercury were placed on the specimen. Both the aluminum and steel were

[3]Kapp, J. A., "The Combined Effects of Mean Stress and Aggressive Environments on Fatigue Crack Growth," ARLCB-TR-82012, ARRADCOM, Benet Weapons Laboratory, Watervliet, NY, May 1982.

difficult to wet. This problem was overcome by electroplating these samples with copper[8] and wetting the copper with mercury in the same manner as described above for brass. Fatigue cracking of the wetted copper coating resulted in wetting and embrittlement of the bulk metal.

RESULTS

Crack Growth Phenomena in 6061-T651

The results of the fatigue crack growth tests for 6061-T651 are shown in Figure 2. The behavior is not unlike the effects of hydrogen on fatigue crack growth on steel.[2] Below a critical value of ΔK (the applied stress intensity factor range), there is no effect of the mercury on fatigue crack growth. Above this critical value (about 7 MPa$\sqrt{m}$), the log of the crack growth rate seems to be nearly linearly related to the log of ΔK initially. Once ΔK reaches about 10-12 MPa$\sqrt{m}$, the crack growth rate increases much less rapidly with increasing ΔK. The crack growth rate in mercury is as much as two orders of magnitude faster at a loading frequency 5 Hz when compared to the air data. Also, the results of the air tests indicate that the crack growth rate is related to ΔK by the Paris power law.

There is an effect of loading frequency on fatigue crack growth rates. Cracks grow faster at low frequency than high frequency. At ΔK of about 20 MPa$\sqrt{m}$, the crack growth rate is about $2\text{-}3\times10^{-5}$ m/cycle and $3\text{-}4\times10^{-4}$ m/cycle

---

[2]Wei, R. P., "On Understanding Environment-Enhanced Fatigue Crack Growth - A Fundamental Approach," ASTM STP 675, J. T. Fong, Ed., American Society for Testing and Materials, 1979, pp. 816-840.

[8]Private Communication, M. H. Kamdar, ARRADCOM, Benet Weapons Laboratory, Watervliet, NY, March 1979.

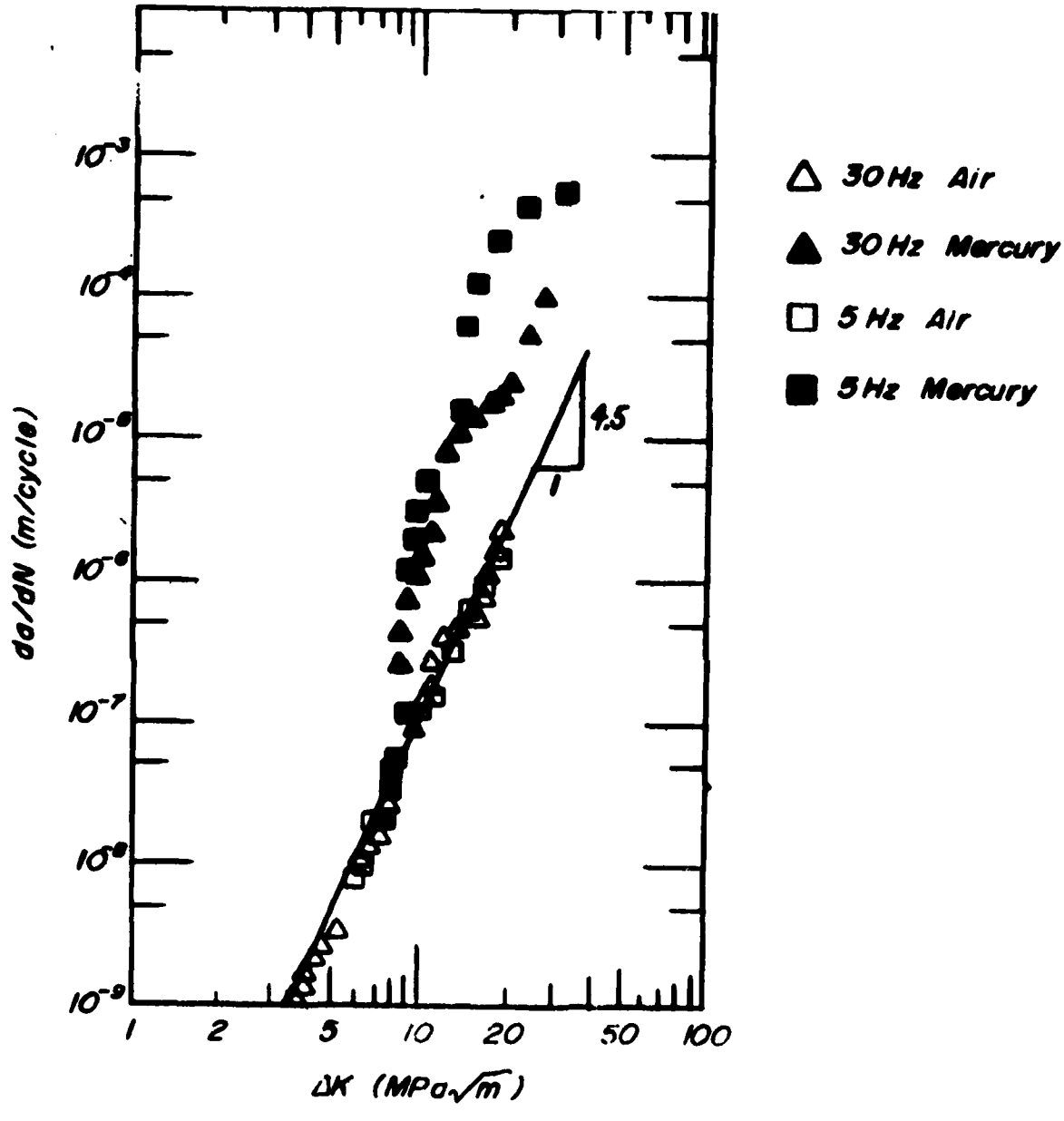

Figure 2. Crack growth behavior in 6061-T651 aluminum under cyclic loading conditions at ambient temperatures.

for 30 Hz and 5 Hz respectively. This is the expected trend, an inverse relationship between crack growth rate and frequency. Such a connection suggests that the time at which the crack is subjected to both mercury and K level is the factor which limits the rate of crack growth. Thus, the use of a simple superposition model may be used to model the fatigue crack growth behavior. The modeling will be discussed further in a later section.

The results of the static loading test for 6061-T651 are shown in Figure 3. In the load control experiment, the embrittled specimen was slowly loaded to a K value at which the crack began to grow. The load was then held constant until total fracture of specimen occurred. In the displacement control test, the CMOD was increased very quickly to produce a high initial K. The displacement was then held constant which resulted in a relaxation of the load, and the crack arrested.

The data show that there is an apparent threshold below which cracks do not grow under displacement control conditions. When K is above this threshold value, the crack growth rate increases with increasing K until the crack velocity reaches above 5 mm/s and remains constant. The threshold behavior is not clearly visible in the load control test. There seems to be no embrittled crack growth when K is less than about 13 MPa$\sqrt{m}$. At K values greater than 13 MPa$\sqrt{m}$ the crack velocity increases to a constant rate of about 4-5 cm/s; about an order of magnitude faster than the displacement control test.

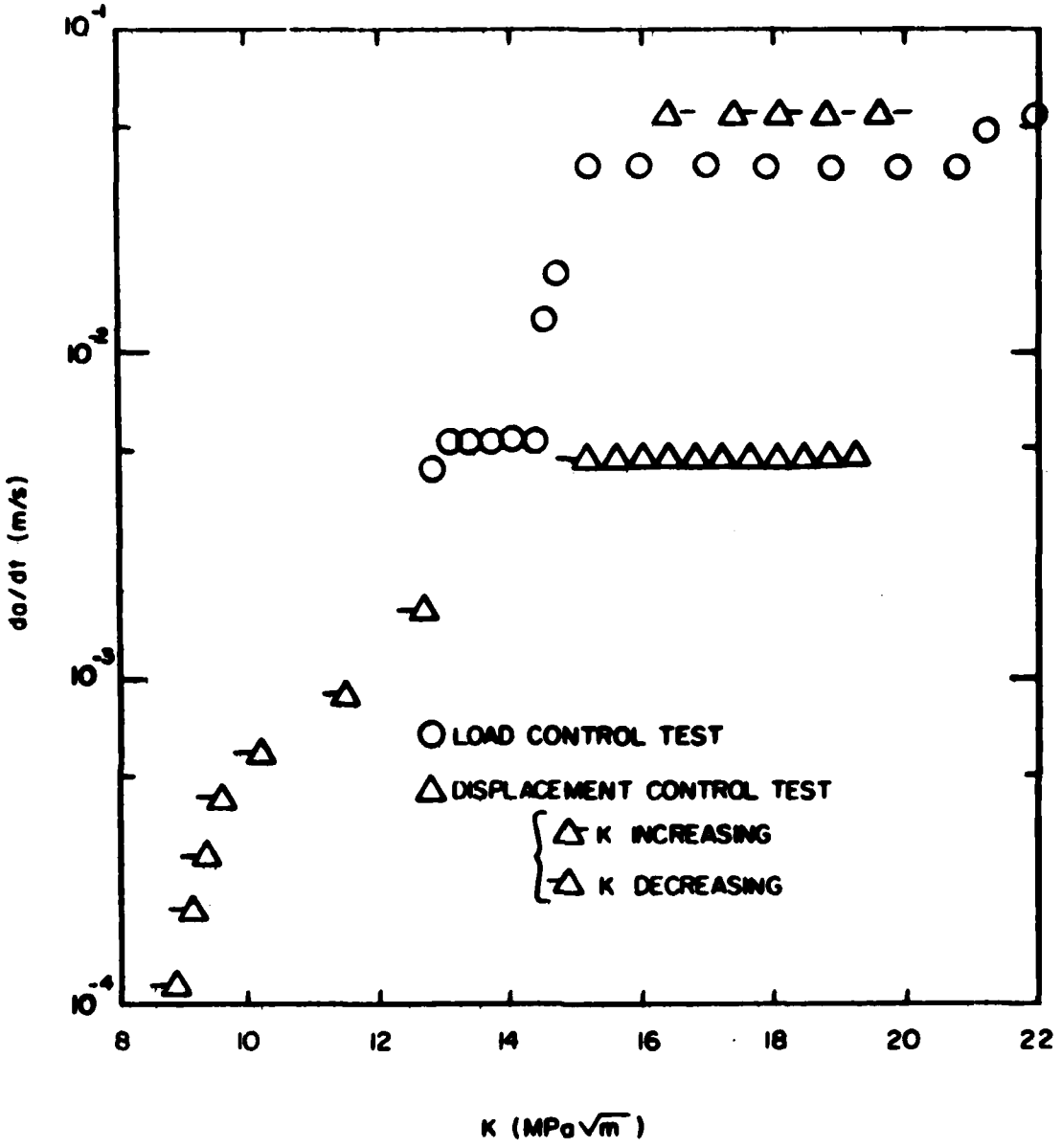

Figure 3. Crack growth behavior in 6061-T651 aluminum under static loading conditions at ambient temperatures.

Examples of more than one crack velocity plateau are given in Spiedel's report.[9] The phenomena is attributed to more than one chemical rate controlling process operating. In the case of the aluminum-mercury couple, it is unlikely that multiple rate limiting processes operate. Rather, the effect shown in Figure 3 is more likely the result of reduced access of the mercury to the crack tip in the displacement control test.

Two factors dealing with the crack surface displacement near the crack tip can restrict the flow of the mercury. In the load control test, K is always increasing. The crack surface displacement is thus ever increasing. Under displacement control conditions, K is first high then decreases. The crack surface displacements are large then decrease. Probably more important than these elastic displacements is the effect of plastic deformation on crack surface displacement.

It is well known that crack closure often occurs during fatigue crack growth tests in many aluminum alloys.[10] There is no reason to believe that a similar phenomena does not occur during the displacement control tests reported for 6061-T651. While the crack tip is unloaded, the crack surfaces consisting of previously deformed material, will close down to form a relatively small capillary, this limiting the access of the liquid mercury to the crack tip.

---

[9]Spiedel, M. O., "Current Understanding of Stress Corrosion Crack Growth in Aluminum Alloys," The Theory of Stress Corrosion Cracking in Alloys, J. Scully, Ed., NATO Scientific Affairs Division, Brussels, 1971.

[10]Elber, Wolf, "The Significance of Fatigue Crack Closure," ASTM STP 486, The American Society of Testing and Materials, 1971, pp. 230-242.

Rate Controlling Processes in Mercury Embrittlement

Two studies have been performed to determine the effect of temperature on cracking.[4,5] The first study deals with fatigue crack growth and static loading crack growth in 6061-T651 in mercury at several temperatures. The second deals with the static loading crack growth of 70/30 alpha brass in mercury. The static test results will be presented first.

Figure 4 shows the results for 6061-T651 at several temperatures, and Figure 5 shows the results for brass. The aluminum measurements show that at all temperatures there is a hysteresis of crack velocity with loading condition. In load control, the crack velocity is always about an order of magnitude faster than in displacement control. But at the lower temperatures, the difference in velocity is less than at higher temperatures. For example, at +25°C, the load control crack velocity is about 4-6 cm/sec, and the displacement control crack velocity is about 5 mm/sec; while the -25°C test results show that the load control crack velocity is nearly 10 cm/sec, but the displacement control velocity is about 2 cm/sec. Also, at high temperature, the crack grow slower than at low temperature.

There are two major differences shown in the brass results. There is no effect of loading condition on crack velocity suggesting that there is always access of the liquid mercury to the crack tip. Second, the effect of temperature is opposite from the 6061-T651 results. Cracks grow faster at high temperature than at low temperature. This indicates that a different rate controlling process is limiting the rate of cracking in these two LME couples.

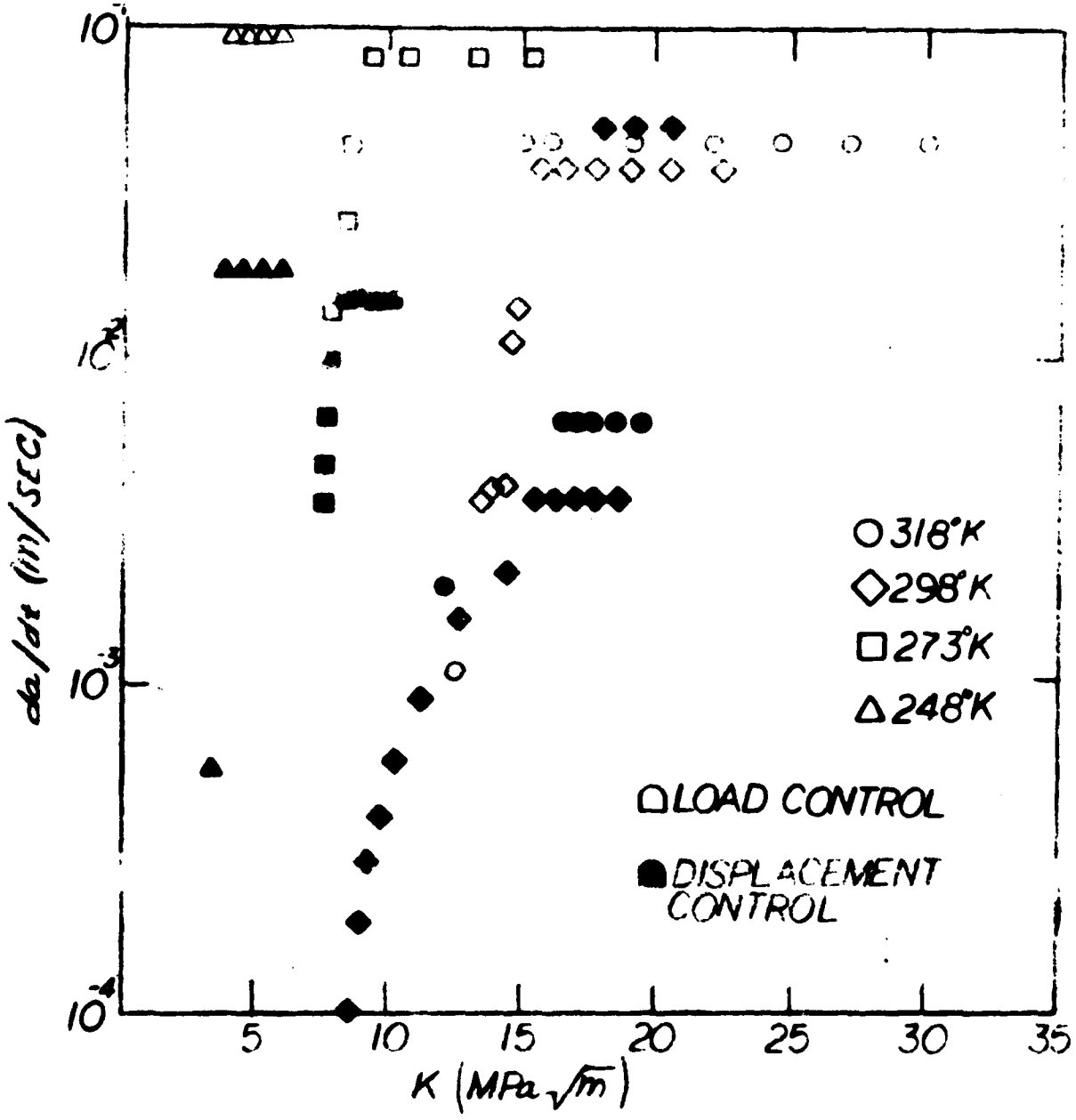

Figure 4. The effect of temperature on crack growth in 6061-T651 aluminum under static loading conditions.

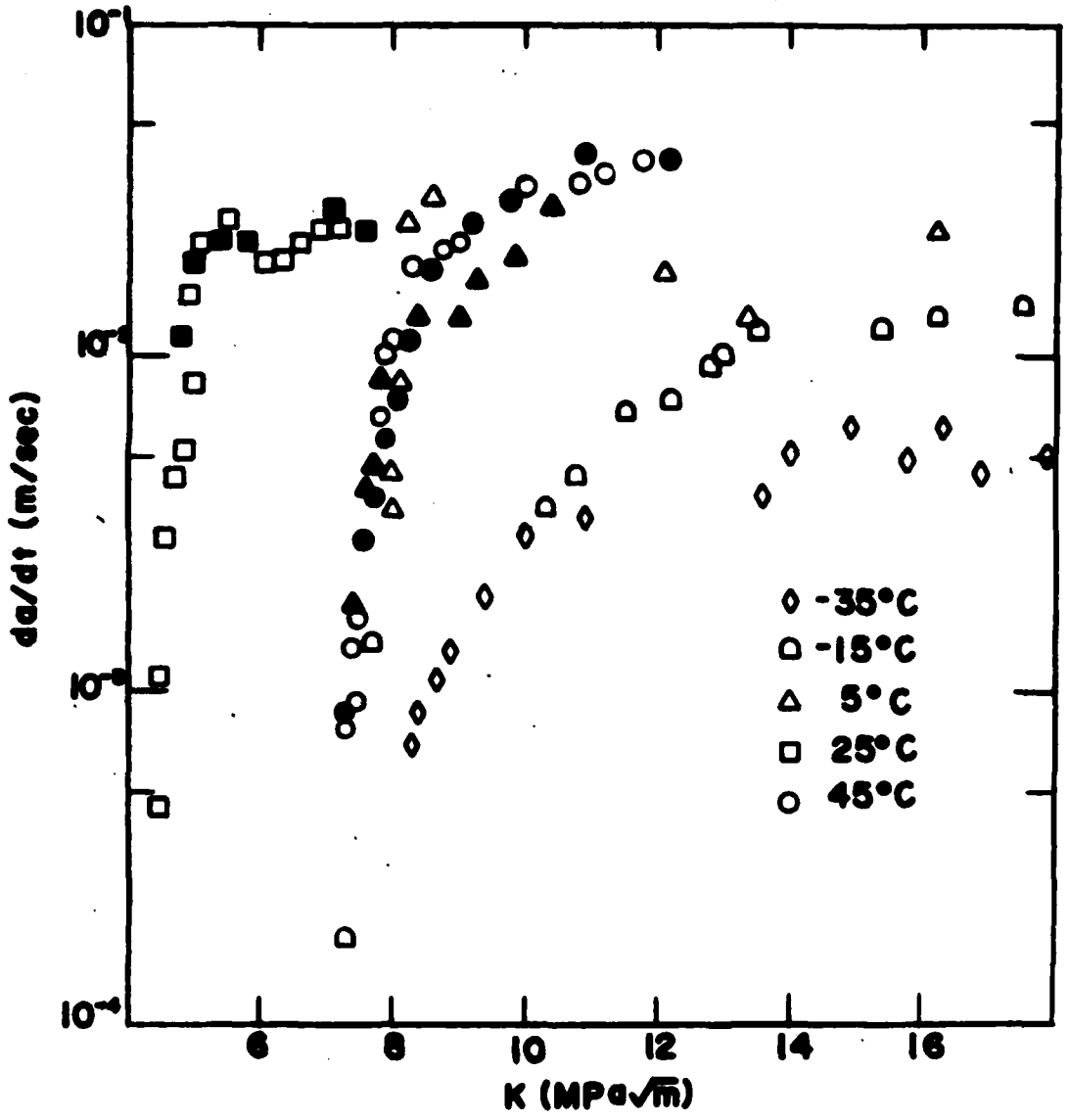

Figure 5. Crack growth under static loading conditions in 70/30 alpha brass at various temperatures.

The effect of temperature on fatigue crack growth rate is somewhat more difficult to determine than in the case of static loading. Since fatigue cracks will propagate without the liquid mercury present, there is an inert environment contribution to the measured total crack growth rate. We wish to determine the effect of temperature on only the mercury component of the crack growth rate. Therefore, the following relationship between the three components is assumed

$$\left(\frac{da}{dN}\right)_{tot} = \left(\frac{da}{dN}\right)_{inert} + \left(\frac{da}{dN}\right)_{Hg} \quad (1)$$

Where $(da/dN)_{tot}$ is the measured crack growth rate, $(da/dN)_{inert}$ is the inert component of crack growth, assumed to be the Paris power law property of 6061-T651 at +25°C in laboratory air, and $(da/dN)_{Hg}$ is the environmental component of interest.

A plot of $(da/dN)_{Hg}$ versus ΔK at three temperatures is given in Figure 6 for 6061-T651. The data fall on three straight lines of different slopes. This fact suggests that the slopes of these lines may be considered as a rate constant similar to the actual crack velocity measurements in static loading. A small slope indicates a slow rate of reaction and a large slope, a fast reaction rate. From Figure 6 it is clear that cracking occurs faster at low temperatures.

The results shown in Figures 4, 5, and 6 can be used to determine an activation energy of liquid metal cracking. This energy is related to the slope of a plot of the log (reaction rate) versus inverse temperature as shown in Figure 7. This graph shows that regardless of loading condition, the activation energy of mercury cracking of 6061-T651 is between +2 and +3 kcal/

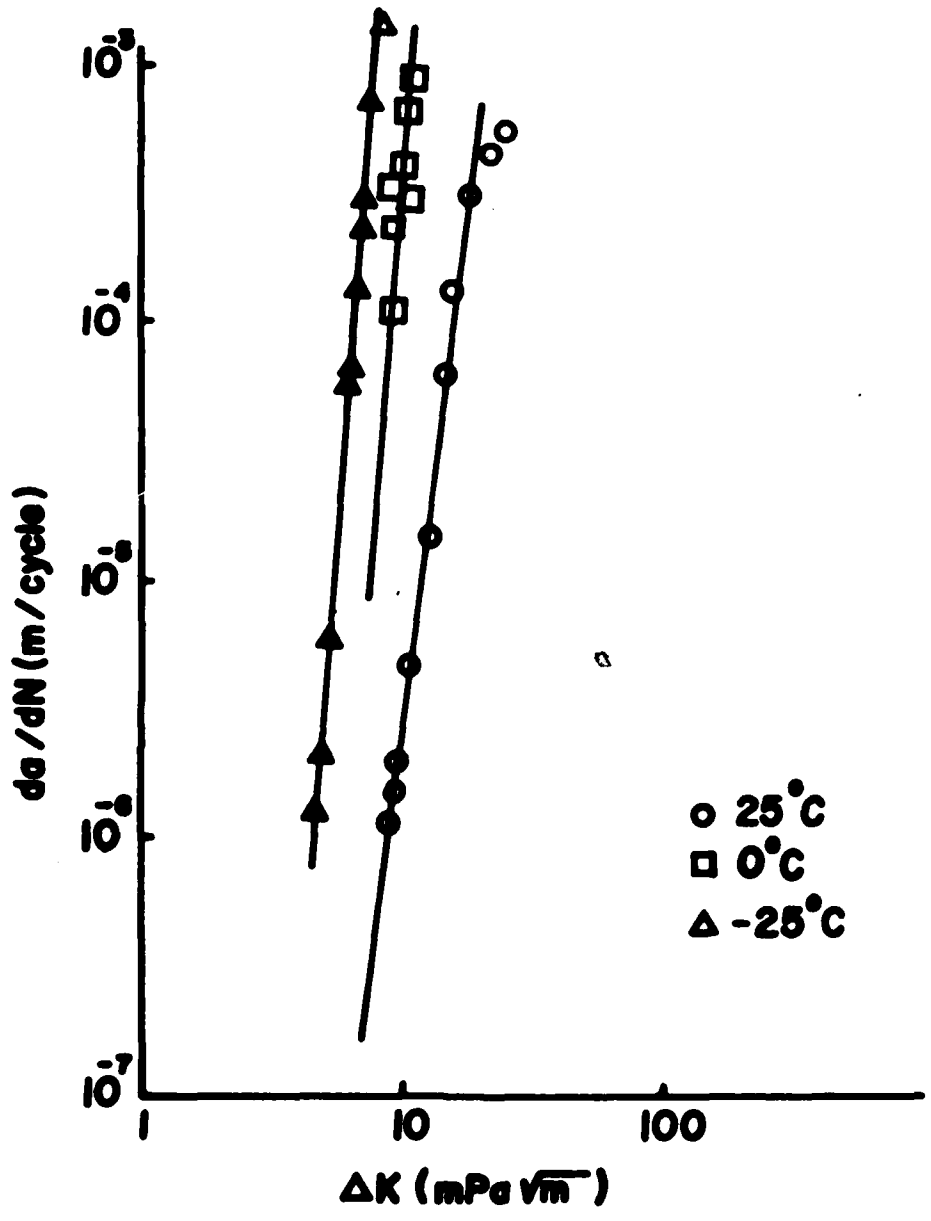

Figure 6. The environmental component of crack growth under cyclic loading at various temperatures.

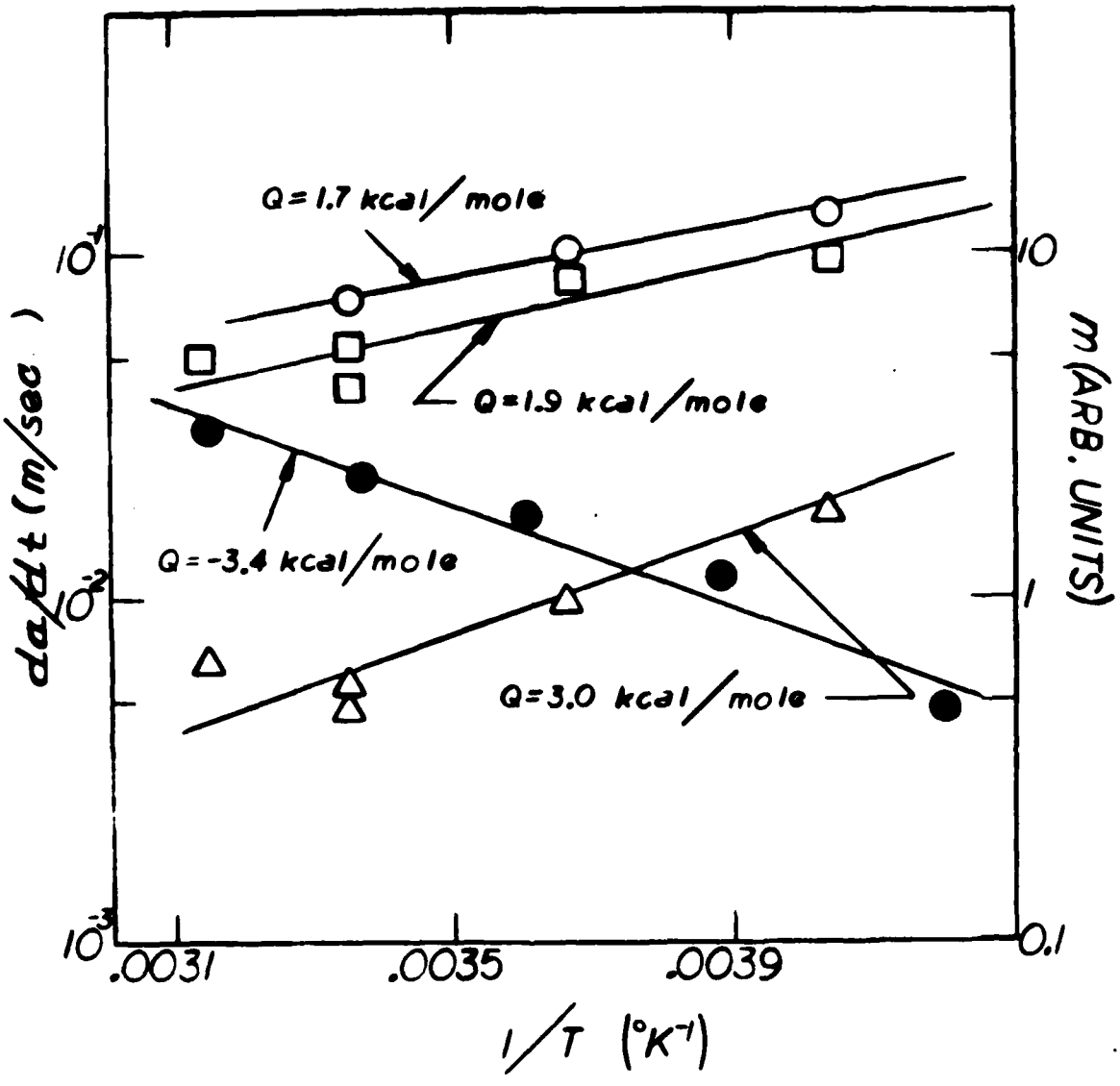

Figure 7. Plot used to determine the activation energy of crack growth. The open circles are for cyclic loading of 6061-T651 aluminum, the squares and triangles are the fixed load and fixed displacement static loading results for 6061-T651 aluminum respectively, and the filled circles are from the 70/30 alpha brass.

mole. The same measurement for the brass-mercury tests show an activation energy of about -3.5 kcal/mole. As stated above, the measurements indicate that there are at least two rate controlling processes which operate in LME. It had been thought that either surface diffusion or vapor transport could be rate limiting.[11] In the case of the former an activation energy of about -2 kcal/mole would be expected, while vapor transport would have an activation energy of about -20 kcal/mole. It is not unreasonable to expect that surface diffusion is limiting the rate of crack growth in the brass/mercury system, but neither surface diffusion nor vapor transport can explain the aluminum results.

One possible explanation of the unusual temperature effects in 6061-T651 is surface adsorption.[5] It is well known that adsorption reactions occur faster at low temperatures than at high temperatures.[12] Furthermore, using a Lennard-Jones potential method, the activation energy of adsorption of mercury on aluminum is estimated to be about +3.5 kcal/mole, which is of the same order of magnitude measured.

---

[5]Kapp, J. A., "Crack Growth in Mercury Embrittled Aluminum Alloys Under Static and Cyclic Loading Conditions," Ph.D. Thesis, Rensselaer Polytechnic Institute, Troy, NY, 1982.

[11]Gordon, P., "Metal Induced Embrittlement of Metals - An Evaluation of Embrittler Transport Mechanisms," Met. Trans. A, Vol. 9A, February 1978, pp. 267-273.

[12]Ross, S. and Olivier, J. P., On Physical Adsorption, John Wiley & Sons, Inc., New York, 1964.

Models For Fatigue Crack Propagation

Two studies have dealt with the development of mathematical expressions for fatigue crack propagation.[3,5] In both instances, a generalized form of the superposition model suggested by Wei and Landes[13] is applied as a first approximation. The model assumes that the total increment of crack advance is given by Eq. (1). The inert component is the Paris power law. The environmental component is a function of the stress ratio or K ratio R ($R = K_{min}/K_{max}$), wave form, frequency and ΔK. Further, this second component is calculated by assuming that when the magnitude of K during a fatigue cycle is less than a critical value (K_{ILME}), the environmental component is zero. Whenever the value of K exceeds K_{ILME}, the crack takes on an instantaneous characteristic velocity v*. Thus, the environmental increment of crack growth during a single fatigue cycle is the time at which K is greater than K_{ILME} times the velocity v*. This results in a three stage representation of crack propagation rate: no environmental component ($K_{max} < K_{ILME}$); a partial environmental effect ($K_{max} > K_{ILME}$, $K_{min} < K_{ILME}$); and the full effect region ($K_{min} > K_{ILME}$). For the case of sinusoidal loading at a frequency f, the crack propagation rate is given as:[3]

---

[3]Kapp, J. A., "The Combined Effects of Mean Stress and Aggressive Environments on Fatigue Crack Growth," ARLCB-TR-82012, ARRADCOM, Benet Weapons Laboratory, Watervliet, NY, May 1982.

[5]Kapp. J. A., "Crack Growth in Mercury Embrittled Aluminum Alloys Under Static and Cyclic Loading Conditions," Ph.D. Thesis, Rensselaer Polytechnic Institute, Troy, Ny, 1982.

[13]Wei, R. P. and Landes, J. D., "Correlation Between Sustained-Load and Fatigue Crack Growth in High Strength Steels," Matls. Res. and Stds., Vol. 9, No. 7, 1969, pp. 25-28.

$$C\Delta K^m \qquad \frac{\Delta K}{(1-R)} \leq K_{ILME}$$

$$\frac{da}{dN} = C\Delta K^m + \frac{v^*}{f}\left[1 - \frac{1}{\pi}\arccos\left[\frac{(1+R)}{(1-R)} - \frac{2K_{ISCC}}{\Delta K}\right]\right] \qquad (2)$$

$$\frac{R\Delta K}{(1-R)} \leq K_{ISCC} \leq \frac{\Delta K}{(1-R)}$$

$$C\Delta K^m + \frac{v^*}{f} \qquad K_{ISCC} \leq \frac{R\Delta K}{(1-R)}$$

There are four constants to evaluate in describing crack growth rates with Eq. (2): C, m, v*, and K_{ILME}. The first two constants are the Paris power law parameters determined by conducting tests in an inert environment. The value of K_{ILME} is easily calculated by performing a zero to tension test in environment. In this case, R = 0 and that value of ΔK at which the crack growth rate deviates from the power law is then K_{ILME}. Finally, v* is determined by fitting Eq. (2) with all other constants defined to a set of data at constant R and f.

Using the 30 Hz data to calculate v* for the 6061-T651, we find K_{ILME} to be about 8 $MPa\sqrt{m}$ and v* to be about 3.6×10^{-4} m/sec. With these values Eq. (2) is plotted in Figure 8 and compared with the actual data from which several observations are made. K_{ILME} determined in the fatigue test is in excellent agreement with the threshold K value from the displacement control static loading test for the same alloy at the same temperature. The characteristic crack velocity v* necessary to obtain a good fit with the actual data is substantially less than the velocities measured in the static loading tests. This suggests that at a given instant during cyclic loading,

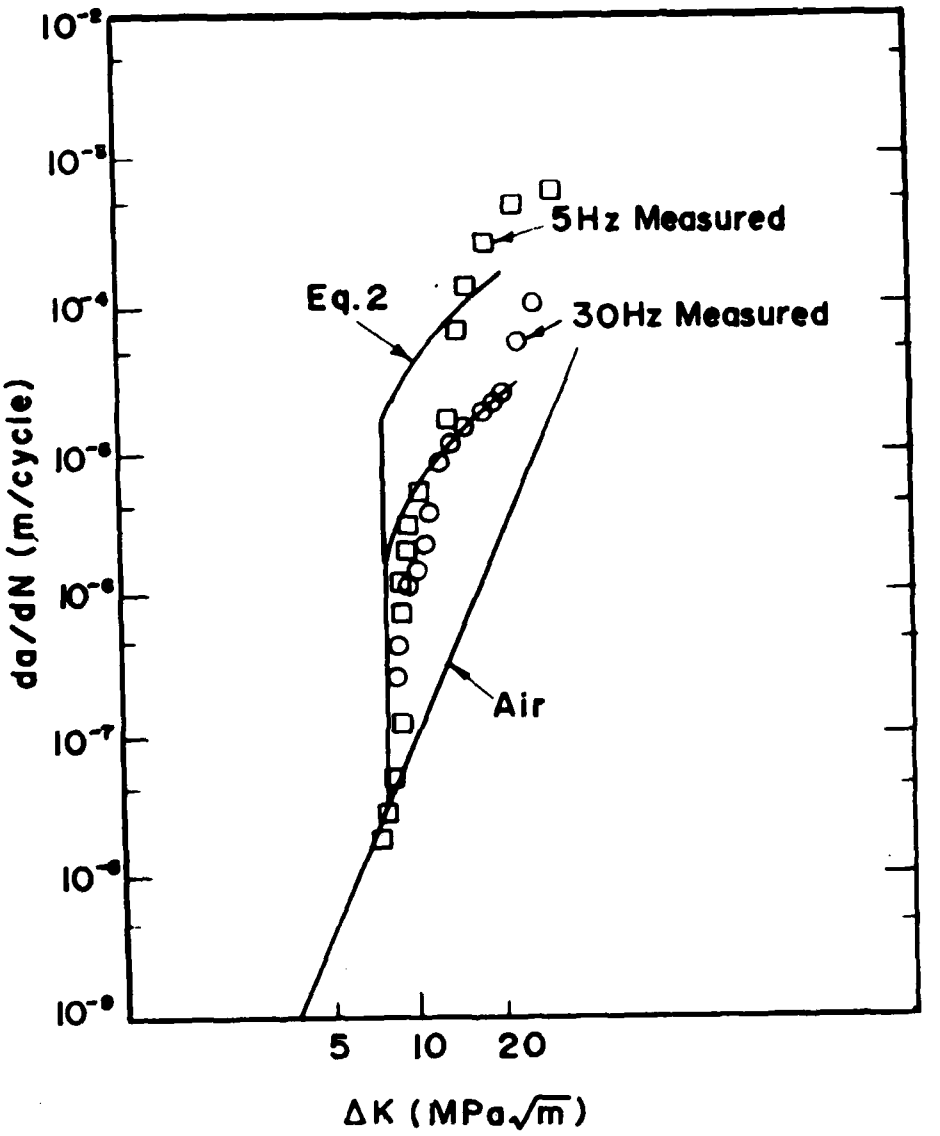

Figure 8. Comparison of Equation (2) with the actual cyclic loading data for 6061-T651 aluminum.

the crack does not grow as quickly as when it is subjected to static loading. Finally Eq. (2) underestimates the actual crack growth rate behavior occurring at 5 Hz. These findings show clearly that maximum effect of liquid mercury embrittlement of a pre-existing crack occurs under static loading.

To examine the effects of K ratio on fatigue crack propagation the results given in Reference 3 for mercury embrittlement of steel are shown in Figure 9. The results for R = 0 are used to determine K_{ILME} and v* in this case. The comparison indicates that when R is zero or negative, the actual data is very well approximated with Eq. (2). But when R is positive the actual behavior can be grossly overestimated. The interesting point to make with these data are that for a compression-tension or a zero-tension cycle, the minimum K during a cycle can never exceed K_{ILME}. Regardless of the applied ΔK, the full effect of the environment can never be attained. The model handles this very well. If the cycle is a tension-tension cycle, or a positive K ratio, the full effect of the environment is predicted to take place, since the minimum K can be greater than K_{ILME}. The data shown in Figure 8 indicates that the full environmental effect is not observed. The reason for this could be an inability of the liquid mercury to be present at the crack tip for sufficient time to cause full embrittlement, but at this writing, the reasons for the unusual behavior under cyclic loading have not been fully addressed.

---

[3]Kapp, J. A., "The Combined Effects of Mean Stress and Aggressive Environments on Fatigue Crack Growth," ARLCB-TR-82012, ARRADCOM, Benet Weapons Laboratory, Watervliet, NY, May 1982.

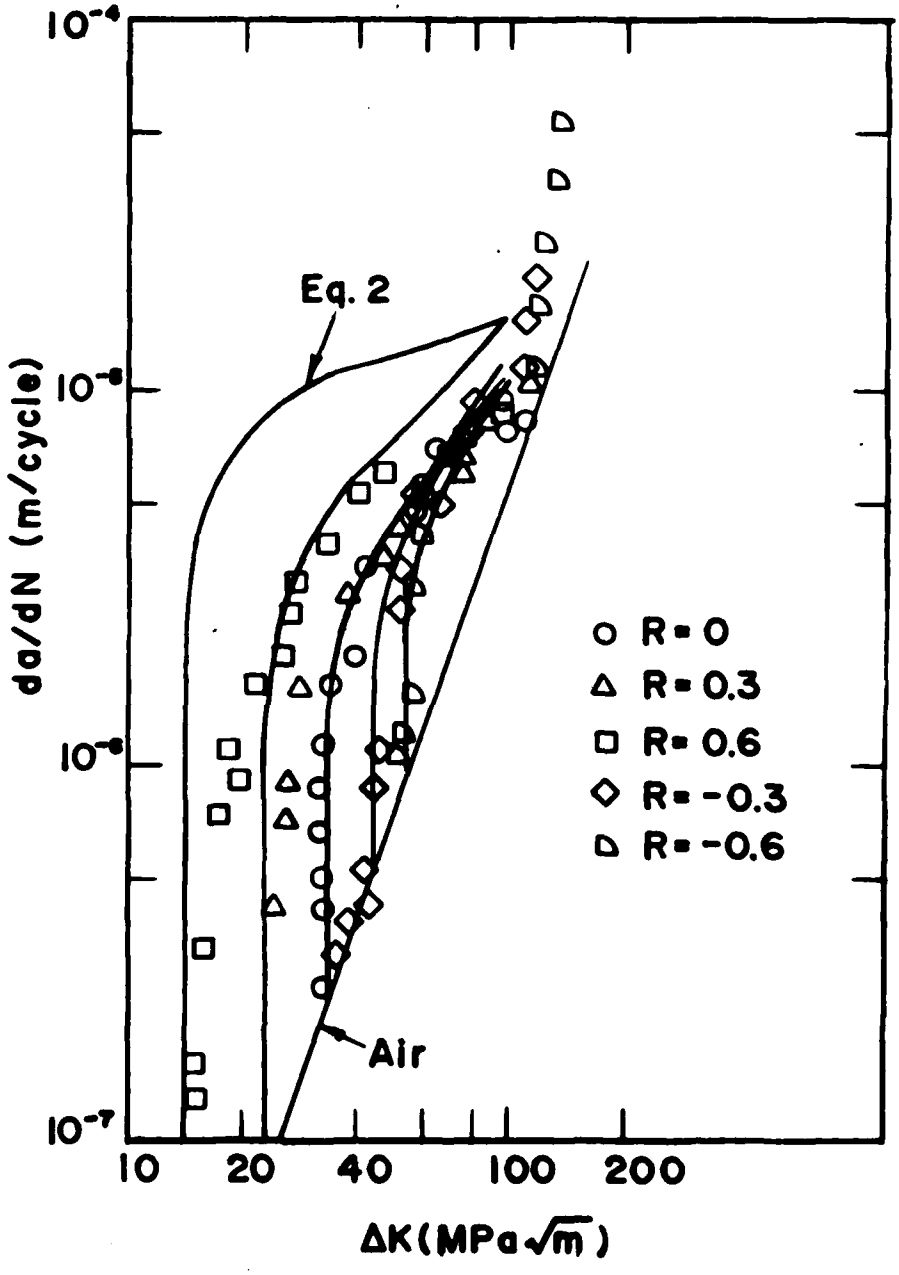

Figure 9. Crack growth at various K ratios in a Ni-Cr-Mo high strength steel compared with Equation (2).

Mode III Crack Initiation Tests

Mode III tearing can offer interesting insights to material behavior under pure shear loading. The solution for the stresses near a blunted crack tip radius ρ is:[14]

$$\tau_{xz} = \frac{-K_{III}}{\sqrt{2\pi r}} \sin \frac{\theta}{2}$$

$$\tau_{yz} = \frac{K_{III}}{\sqrt{2\pi r}} \sin \frac{\theta}{2} \qquad (3)$$

where r and θ are measured as shown in Figure 10.

It is readily seen that the stresses at the root of a notch in pure torison are pure shear. Therefore, this loading condition may enable us to compare two mechanisms of LME under unique circumstances. The two mechanisms are decohesion[15,16] and enhanced shear.[17] An absolute requisite for decohesion is tensile stresses at the crack tip. In Mode III loading tensile stresses do not exist. If a test were performed where liquid mercury is carefully placed only at a notch tip loaded in Mode III, decohesion can not possibly contribute to any embrittlement. Furthermore, if enhanced shear operates, embrittlement should occur readily, and the crack should advance totally in the plane of the notch, since that is the plane of maximum shear stress.

---

[14]Creager, M. and Paris, P. C., "Elastic Field Equations for Blunt Cracks With Reference to Stress Corrosion Cracking," Int. J. of Fracture Mechanics, Vol. 3, No. 4, December 1967, pp. 247-252.

[15]Stoloff, N. S. and Johnston, T. L., "Crack Propagation in a Liquid Metal Environment," Acta. Metallurgica, Vol. 11, April 1963, pp. 251-256.

[16]Westwood, A. R. C. and Kamdar, M. H., "Concerning Liquid Metal Embrittlement, Particularly of Zinc Monocrystals by Mercury," Phil. Mag., Vol. 8, 1963, pp. 787-804.

[17]Lynch, S. P., "Liquid Metal Embrittlement in an Al 6% Zn 3% Mg Alloy," Acta. Metallurgica, Vol. 29, 1981, pp. 325-340.

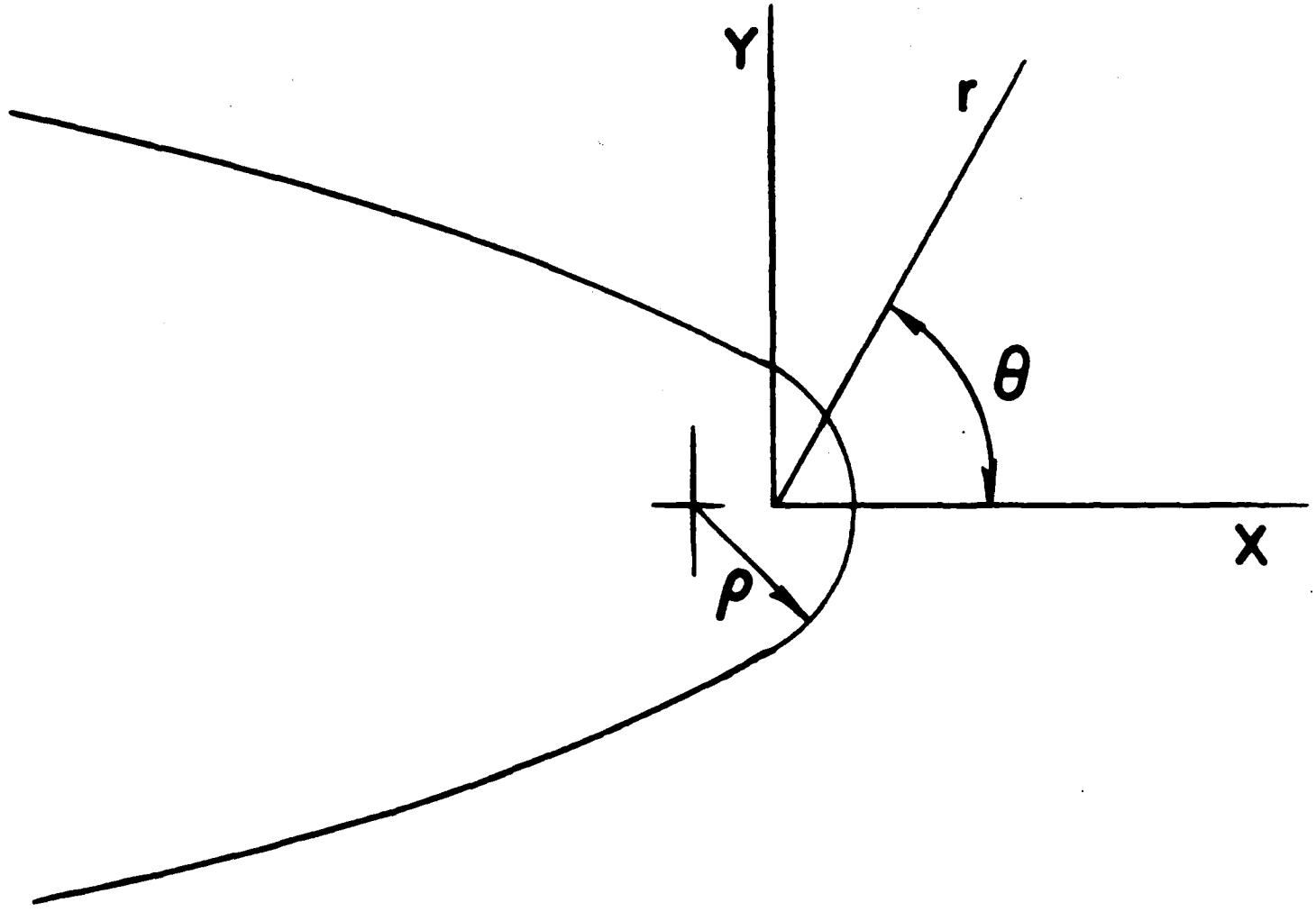

Figure 10. Coordinate system for the near field of a blunt crack tip.

Such tests were performed with 70/30 alpha brass wetted with liquid mercury. The results presented as simple torque-twist diagrams are given in Figure 11. The tests conducted in air indicate a ductile shear fracture. The tests in mercury show clearly that embrittlement readily occurs under these loading conditions. The macroscopic appearance of the fracture, Figure 12, reveals that the total fracture event in mercury did not occur under pure shear conditions, rather most of the cracking occurred on a helix oriented about 45° from the plane of the notch. The helix is the location of the maximum tensile stresses.

These results immediately suggest two conclusions. First, the presence of mercury significantly enhances the likelihood of crack initiation under pure shear loading. With no mercury present, about 70° of twist is required to cause crack initiation, but with mercury, Mode III crack initiation occurs with less than 10° of twist. Second, once a crack is formed, the crack changes direction to orient itself in the direction of the maximum tensile normal stress. These observations are further strengthened by micrograph shown in Figure 13. The polished and etched transverse section shows that crack initiation indeed takes place at the notch tip in essentially the plane of the notch. After the crack initiates it grows only a very short distance under pure Mode III conditions and changes direction to grow under conditions where tensile stresses are maximum.

These test results do not resolve the controversy surrounding the micro-mechanism of LME. They do indicate that there is enhanced shear from the presence of the liquid in crack initiation. But, if enhanced shear is the mechanism of crack propagation, why do cracks change planes to orient

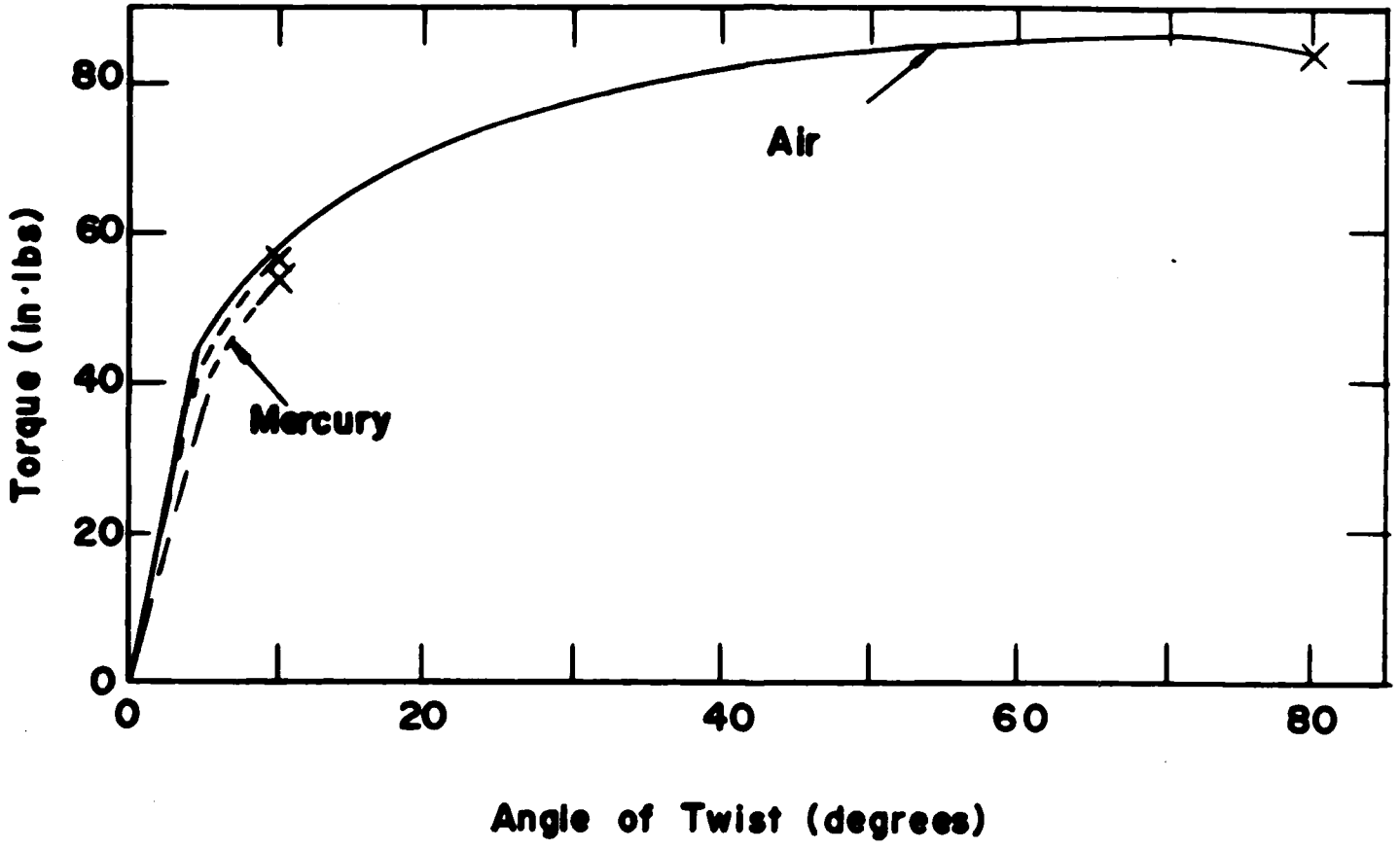

Figure 11. Torque-twist diagram for Mode III crack initiation in 70/30 alpha brass.

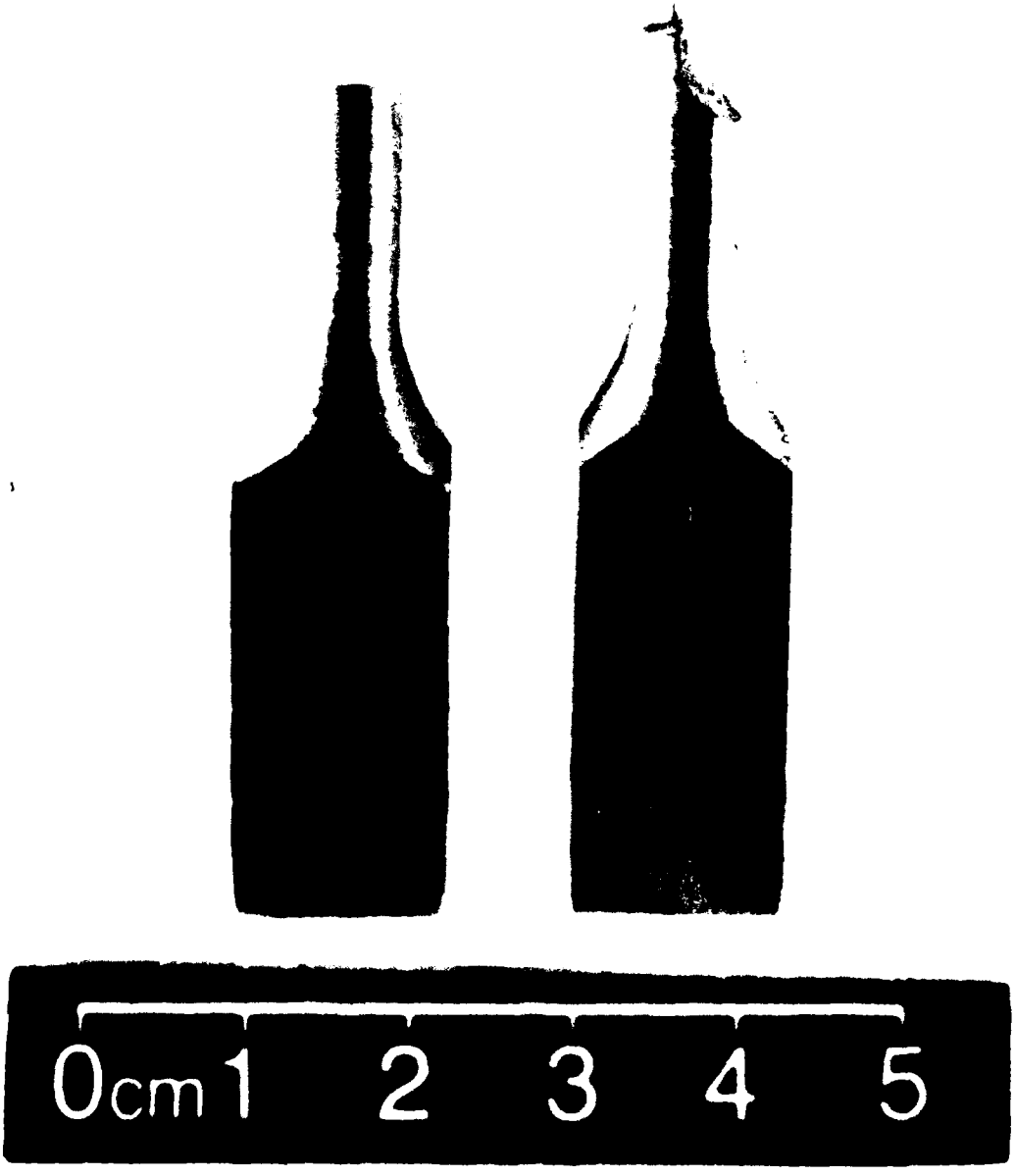

Figure 12. Macroscopic fracture appearance of 70/30 alpha brass under Mode III conditions. The specimen on the left was broken in air, the one on the right was broken in mercury.

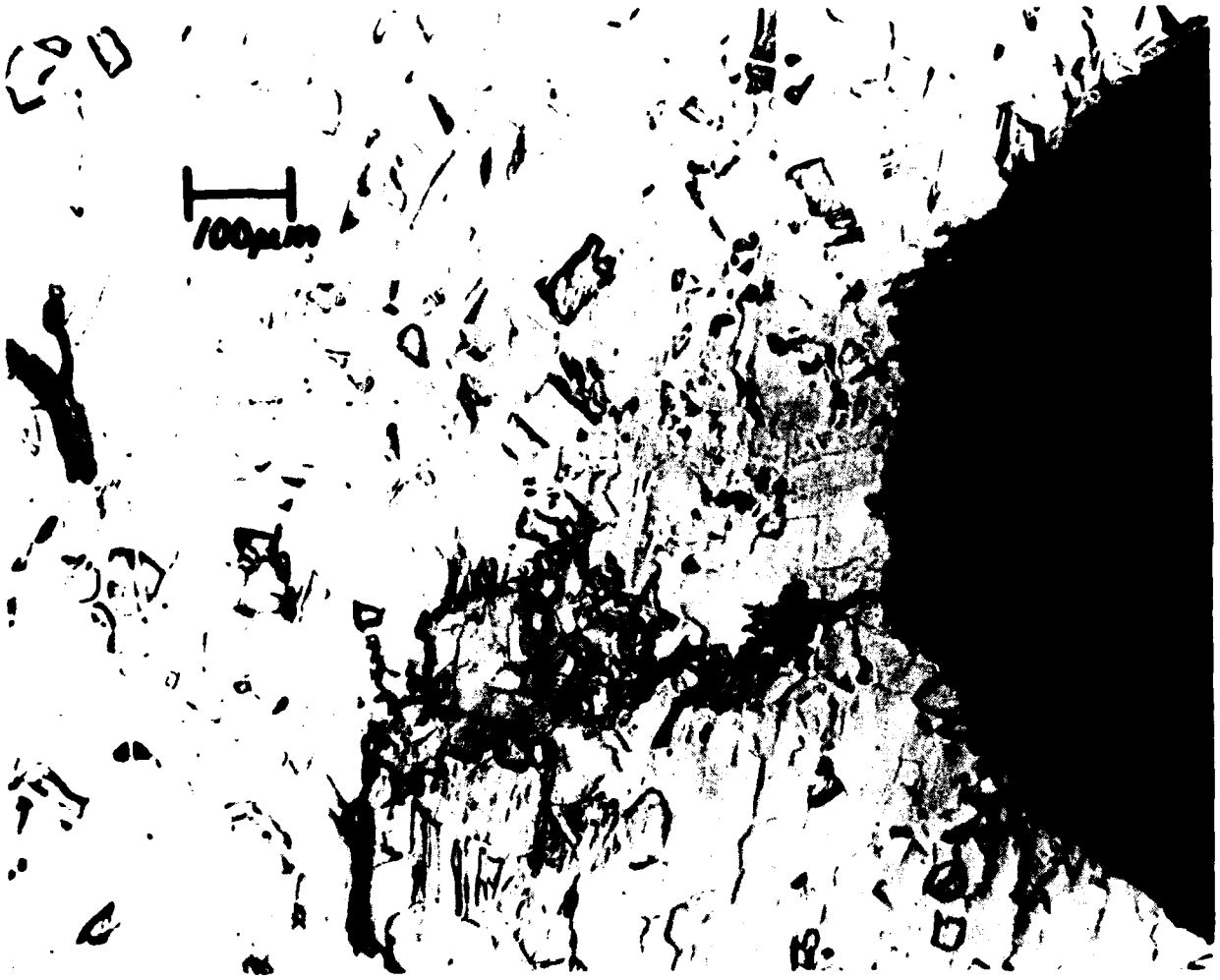

Figure 13. Transverse section of the vicinity of the notch tip for 70/30 alpha brass showing pure shear crack initiation and crack growth in the plane of maximum tensile stress.

themselves in the direction of the maximum tensile stress? It is well known that shear stresses do exist at the tip of Mode I crack and enhanced shear may contribute to the propagation of such cracks. But it seems to this writer that cracks strive to propagate along a path where tensile stresses are the highest and thus, the greatest effect from decohesion obtained.

SUMMARY AND CONCLUSION

A significant amount of fracture mechanics testing in the mercury embrittlement of metals has been performed. The results of the tests show that cracks apparently grow faster under static loading than under cyclic loading. In some cases, crack velocity is a function of static loading condition (fixed load or fixed displacement). Testing at several temperatures indicate that at least two rate controlling processes govern the rate of crack propagation. These are surface adsorption in the aluminum/mercury system and surface diffusion in the brass/mercury system. A simple model for fatigue crack propagation in mercury shows that the effects of loading frequency can be adequately modeled, but the effects of mean stress on K ratio are only accounted for in some cases. Testing in Mode III indicates that the enhanced shear mechanism significantly contributes to crack initiation in the brass/mercury system, but decohesion probably dominates crack propagation.

REFERENCES

1. Clark, W. G. Jr., "Effect of Temperature and Pressure on Hydrogen Cracking in High Strength Type 4340 Steel," J. Materials for Engineering Systems, Vol. 1, June 1979, pp. 33-40.
2. Wei, R. P., "On Understanding Environment-Enhanced Fatigue Crack Growth - A Fundamental Approach," ASTM STP 675, J. T. Fong, Ed., American Society for Testing and Materials, 1979, pp. 816-840.
3. Kapp, J. A., "The Combined Effects of Mean Stress and Aggressive Environments on Fatigue Crack Growth," ARLCB-TR-82012, ARRADCOM, Benet Weapons Laboratory, Watervliet, NY, May 1982.
4. Kamdar, M. H., "The Role of Liquid in the Mechanics of Crack Growth in LME," in progress.
5. Kapp, J. A., "Crack Growth in Mercury Embrittled Aluminum Alloys Under Static and Cyclic Loading Conditions," Ph.D. Thesis, Rensselaer Polytechnic Institute, Troy, NY, 1982.
6. Tada, H., Paris, P. C., and Irwin, G. R., The Stress Analysis of Cracks Handbook, Del Research Corporation, Hellertown, PA, 1973.
7. Yoder, G. R., Cooley, L. A., and Crooker, T. W., "Procedures for Precision Measurement of Fatigue Crack Growth Rate Using Crack-Opening Displacement Techniques," ASTM STP 738, S. J. Hudak and R. J. Bucci, Eds., American Society for Testing and Materials, 1981, pp. 85-102.
8. Private Communication, M. H. Kamdar, ARRADCOM, Benet Weapons Laboratory, Watervliet, NY, March 1979.

9. Spiedel, M. O., "Current Understanding of Stress Corrosion Crack Growth in Aluminum Alloys," The Theory of Stress Corrosion Cracking in Alloys, J. Scully, Ed., NATO Scientific Affairs Division, Brussels, 1971.

10. Elber, Wolf, "The Significance of Fatigue Crack Closure," ASTM STP 486, The American Society of Testing and Materials, 1971, pp. 230-242.

11. Gordon, P., "Metal Induced Embrittlement of Metals - An Evaluation of Embrittler Transport Mechanisms," Met. Trans. A, Vol. 9A, February 1978, pp. 267-273.

12. Ross. S. and Olivier, J. P., On Physical Adsorption, John Wiley & Sons, Inc., New York, 1964.

13. Wei, R. P. and Landes, J. D., "Correlation Between Sustained-Load and Fatigue Crack Growth in High Strength Steels," Matls. Res. and Stds., Vol. 9, No. 7, pp. 25-28.

14. Creager, M. and Paris, P. C., "Elastic Field Equations for Blunt Cracks With Reference to Stress Corrosion Cracking," Int. J. of Fracture Mechanics, Vol. 3, No. 4, December 1967, pp. 247-252.

15. Stoloff, N. S. and Johnston, T. L., "Crack Propagation in a Liquid Metal Environment," Acta. Metallurgica, Vol. 11, April 1963, pp. 251-256.

16. Westwood, A. R. C. and Kamdar, M. H., "Concerning Liquid Metal Embrittlement, Particularly of Zinc Monocrystals by Mercury," Phil. Mag., Vol. 8, 1963, pp. 787-804.

17. Lynch, S. P., "Liquid Metal Embrittlement in an Al 6% Zn 3% Mg Alloy," Acta. Metallurgica, Vol. 29, 1981, pp. 325-340.

TECHNICAL REPORT INTERNAL DISTRIBUTION LIST

	NO. OF COPIES
CHIEF, DEVELOPMENT ENGINEERING BRANCH	
ATTN: DRDAR-LCB-D	1
-DP	1
-DR	1
-DS (SYSTEMS)	1
-DS (ICAS GROUP)	1
-DC	1
CHIEF, ENGINEERING SUPPORT BRANCH	
ATTN: DRDAR-LCB-S	1
-SE	1
CHIEF, RESEARCH BRANCH	
ATTN: DRDAR-LCB-R	2
-R (ELLEN FOGARTY)	1
-RA	1
-RM	1
-RP	1
-RT	1
TECHNICAL LIBRARY	5
ATTN: DRDAR-LCB-TL	
TECHNICAL PUBLICATIONS & EDITING UNIT	2
ATTN: DRDAR-LCB-TL	
DIRECTOR, OPERATIONS DIRECTORATE	1
DIRECTOR, PROCUREMENT DIRECTORATE	1
DIRECTOR, PRODUCT ASSURANCE DIRECTORATE	1

NOTE: PLEASE NOTIFY DIRECTOR, BENET WEAPONS LABORATORY, ATTN: DRDAR-LCB-TL, OF ANY REQUIRED CHANGES.

TECHNICAL REPORT EXTERNAL DISTRIBUTION LIST

	NO. OF COPIES
ASST SEC OF THE ARMY RESEARCH & DEVELOPMENT ATTN: DEP FOR SCI & TECH THE PENTAGON WASHINGTON, D.C. 20315	1
COMMANDER DEFENSE TECHNICAL INFO CENTER ATTN: DTIC-DDA CAMERON STATION ALEXANDRIA, VA 22314	12
COMMANDER US ARMY MAT DEV & READ COMD ATTN: DRCDE-SG 5001 EISENHOWER AVE ALEXANDRIA, VA 22333	1
COMMANDER US ARMY ARRADCOM ATTN: DRDAR-LC	1
DRDAR-LCA (PLASTICS TECH EVAL CEN)	1
DRDAR-LCE	1
DRDAR-LCM (BLDG 321)	1
DRDAR-LCS	1
DRDAR-LCU	1
DRDAR-LCW	1
DRDAR-TSS (STINFO) DOVER, NJ 07801	2
DIRECTOR US ARMY BALLISTIC RESEARCH LABORATORY ATTN: DRDAR-TSB-S (STINFO) ABERDEEN PROVING GROUND, MD 21005	1
COMMANDER US ARMY ARRCOM ATTN: DRSAR-LEP-L ROCK ISLAND ARSENAL ROCK ISLAND, IL 61299	1
COMMANDER ROCK ISLAND ARSENAL ATTN: SARRI-ENM (MAT SCI DIV) ROCK ISLAND, IL 61299	1
DIRECTOR US ARMY INDUSTRIAL BASE ENG ACT ATTN: DRXIB-M ROCK ISLAND, IL 61299	1
COMMANDER US ARMY TANK-AUTMV R&D COMD ATTN: TECH LIB - DRSTA-TSL WARREN, MI 48090	1
COMMANDER US ARMY TANK-AUTMV COMD ATTN: DRSTA-RC WARREN, MI 48090	1
COMMANDER US MILITARY ACADEMY ATTN: CHM, MECH ENGR DEPT WEST POINT, NY 10996	1
US ARMY MISSILE COMD REDSTONE SCIENTIFIC INFO CEN ATTN: DOCUMENTS SECT, BLDG 4484 REDSTONE ARSENAL, AL 35898	2
COMMANDER US ARMY FGN SCIENCE & TECH CEN ATTN: DRXST-SD 220 7TH STREET, N.E. CHARLOTTESVILLE, VA 22901	1
COMMANDER US ARMY MATERIALS & MECHANICS RESEARCH CENTER ATTN: TECH LIB - DRXMR-PL WATERTOWN, MA 02172	2

NOTE: PLEASE NOTIFY COMMANDER, ARRADCOM, ATTN: BENET WEAPONS LABORATORY, DRDAR-LCB-TL, WATERVLIET ARSENAL, WATERVLIET, NY 12189, OF ANY REQUIRED CHANGES.

TECHNICAL REPORT EXTERNAL DISTRIBUTION LIST (CONT'D)

	NO. OF COPIES
COMMANDER US ARMY RESEARCH OFFICE ATTN: CHIEF, IPO P.O. BOX 12211 RESEARCH TRIANGLE PARK, NC 27709	1
COMMANDER US ARMY HARRY DIAMOND LAB ATTN: TECH LIB 2800 POWDER MILL ROAD ADELPHIA, MD 20783	1
COMMANDER NAVAL SURFACE WEAPONS CEN ATTN: TECHNICAL LIBRARY CODE X212 DAHLGREN, VA 22448	1
DIRECTOR US NAVAL RESEARCH LAB ATTN: DIR, MECH DIV	1
CODE 26-27 (DOC LIB)	1
WASHINGTON, D.C. 20375	
METALS & CERAMICS INFO CEN BATTELLE COLUMBUS LAB 505 KING AVE COLUMBUS, OH 43201	1
MATERIEL SYSTEMS ANALYSIS ACTV ATTN: DRXSY-MP ABERDEEN PROVING GROUND MARYLAND 21005	1

NOTE: PLEASE NOTIFY COMMANDER, ARRADCOM, ATTN: BENET WEAPONS LABORATORY, DRDAR-LCB-TL, WATERVLIET ARSENAL, WATERVLIET, NY 12189, OF ANY REQUIRED CHANGES.

3